NJC

PAPER

View Article Online
View Journal | View Issue

Cite this: *New J. Chem.*, 2019, **43**, 3513

A colorimetric and "off–on" fluorescent Pd^{2+} chemosensor based on a rhodamine-ampyrone conjugate: synthesis, experimental and theoretical studies along with *in vitro* applications†

Sanchita Mondal,*[a] Saikat Kumar Manna,*[b] Sudipta Pathak,*[b] Abdulla Al Masum[c] and Subrata Mukhopadhyay[a]

Received 12th October 2018,
Accepted 22nd January 2019

DOI: 10.1039/c8nj05194a

rsc.li/njc

We successfully designed and developed a rhodamine based "turn-on" chemosensor **L** for the detection of Pd^{2+} ions down to 1.19×10^{-5} M (11.9 μM). In organo-aqueous solution, probe **L** displayed highly selective and sensitive colorimetric and fluorescence responses toward Pd^{2+} based on the ring-opening mechanism of the rhodamine spirolactam ring upon complexation with Pd^{2+}. In the presence of Pd^{2+} ions, probe **L** formed an **L**–Pd^{2+} complex in 1 : 1 stoichiometry which was confirmed by the Job plot and mass spectroscopy. Moreover, we performed DFT (density functional theory) studies to identify the coordination characteristics and binding nature of **L** and the **L**–Pd^{2+} complex. In addition, cell imaging experiments revealed that probe **L** was able to permeate cells, and able to image Pd^{2+} in living cells.

Introduction

Palladium as one of the most significant platinum group metals (PGMs) is extensively utilized in catalytic converters of automobiles, fuel cells, aircraft spark plugs, blood sugar test strips, groundwater treatment, photography, electrical equipment, and dental crowns and in the production of several surgical instruments.[1–3] Moreover, palladium salts are mostly used as oxidizing agents and efficient metal catalysts for various carbon–carbon and carbon–heteroatom coupling reactions such as the Negishi, Nozaki–Hiyama, Heck, Kumada, Buchwald–Hartwig, Sonogashira, Stille, Tsuji–Trost transformations and Suzuki–Miyaura.[4,5] These Pd-catalyzed coupling reactions are very effective and have found increased popularity for the synthesis and development of drug molecules.[6] However, these reactions present a problem that is even after purification steps, high amounts of residual palladium can sometimes remain in the isolated final product which can be consumed along with the synthesized drugs.[7] Hence, extensive use of palladium species in academic circles and industry, which often liberate a huge amount of palladium to the environment, causes an immense health problem, compromises food safety and also spoils agro-ecosystems.[8] Owing to its thiophilic character, palladium can bind to proteins (silk fibroin, casein, and many enzymes), thiol containing amino acids, vitamin B6, DNA and other macromolecules and thus disturb several cellular processes like degradation of DNA, damaging cell mitochondria and inhibiting enzyme activity.[9,10] Moreover, it is found that excess accumulation of palladium in the human body causes various allergic reactions as well as stomatitis, contact dermatitis, periodontal gum disease and lichinoid reactions and hence palladium species are considered as highly toxic to human health.[11–13] Thus, the permitted concentration of palladium in active pharmaceutical ingredients is strictly limited by governmental restrictions that state it must not exceed 5–10 ppm and the recommended utmost dietary intake of palladium ranges from less than 1.5 μg to 15 μg per person per day.[14] These issues raise the vital need to develop appropriate, highly efficient, selective and sensitive analytical tools for real-time monitoring of palladium species in biological and environmental samples. To date, several conventional analytical methods have been developed for the detection of palladium ions, such as atomic absorption spectroscopy (AAS), solid-phase microextraction high performance liquid chromatography (SPME-HPLC), inductively coupled plasma atomic emission spectrometry (ICP-AES), inductively coupled plasma mass spectrometry, time-of-flight resonance ionisation mass spectrometry, capillary zone electrophoresis and X-ray fluorescence.[15,16] However, these techniques often require large, costly, sophisticated instrumentation, well-trained workers

[a] *Department of Chemistry, Jadavpur University, Kolkata 700032, India. E-mail: mondalsanchita2011@gmail.com*
[b] *Department of Chemistry, Haldia Government College, Debhog, Purba Medinipur, West Bengal 721657, India. E-mail: saikat.manna.chem@gmail.com, sudiptachemster@gmail.com*
[c] *Department of Life Science & Bio-technology, Jadavpur University, Kolkata 700032, India*

† Electronic supplementary information (ESI) available. See DOI: 10.1039/c8nj05194a

and time-consuming sample preparation steps, and they cannot be simply applied in on-line or in-field analysis. Among these conventional techniques, optical detection (fluorometric and colorimetric) methods belonging to the spectroscopy field are more suitable and effective for rapid detection of palladium ions (Pd^{2+}) owing to their easy sample operation, low cost, simplicity, sensitivity, selectivity, rapid response and nondestructive nature.[17] Up to now, several Pd^{2+} chemosensors have been reported; though, most of these demonstrate a fluorescence quenching *i.e.* turn-off response due to its paramagnetic nature.[18,19] However, fluorescence-enhancing *i.e.* turn-on chemosensors would be more efficient, sensitive and reliable for Pd^{2+} detection in solution as well as in living cells.[20]

Some recent "turn-on" fluorescent chemosensors and chemodosimeters for Pd^{2+} ions have been developed, but still highly selective, sensitive and "turn-on" type systems are needed.[21,22] It is noteworthy that Pd^{2+} turn on sensors are not extensively available in the literature. Moreover, most of the reported Pd^{2+} organic sensors were synthesized using complex multistep processes which are quite time consuming and not economical (Table S3, ESI†). In this regard, the rhodamine framework has been commonly utilized for the construction of "off–on" fluorescence probes since rhodamine displays a non-fluorescent spirocyclic form to fluorescent ring-open amide equilibrium during the detection of metal ions.[23,24] Additionally, another benefit of such rhodamine-based sensing platforms is that the ring opening reaction in the presence of metal ions is also accompanied by a color change from colorless to pink which allows metal ion detection with the naked eye. Our method also utilizes only three easily attainable steps in the synthesis with high yield at each step and is relatively much less time demanding.

Keeping the above-mentioned criteria in mind, herein, we designed and synthesized a new rhodamine B based probe **L** which acts as a highly competent colorimetric and "turn-on" fluorescent chemosensor towards Pd^{2+} in CH_3CN–water (4 : 1, v/v, 10 mM HEPES buffer, pH 7.4) solution. Probe **L** demonstrated tremendous sensitivity and selectivity for Pd^{2+} ions over other competing metal ions. Moreover, probe **L** can also be used to image Pd^{2+} in living cells.

Results and discussion

Probe **L** was synthesized in two steps following the route outlined in Scheme 1. Initially, compound **1** was prepared by a condensation reaction between 4-amino antipyrine (ampyrone) and glyoxal with 91% yield.

Finally, chemosensor **L** was synthesized in 84% yield as a yellow solid from rhodamine B by amination with hydrazine hydrate followed by a Schiff base condensation with compound **1** in ethanol solution under reflux conditions. The chemical structure of probe **L** was well characterized by ^1H NMR, ^{13}C NMR, and mass spectroscopy as illustrated in the Experimental section.

The chemosensing behavior of probe **L** toward different metal cations (Na^+, K^+, Mg^{2+}, Ca^{2+}, Sr^{2+}, Ba^{2+}, Cr^{3+}, Mn^{2+}, Fe^{2+}, Fe^{3+}, Co^{2+}, Ni^{2+}, Cu^{2+}, Zn^{2+}, Cd^{2+}, Pb^{2+}, Hg^{2+}, Pd^{2+}, Pd^0, Pt^{2+}, Ru^{3+}, Al^{3+} and Ag^+) and its preferential selectivity and sensitivity toward Pd^{2+} over the other metal ions was examined by absorption and fluorescence titrations.

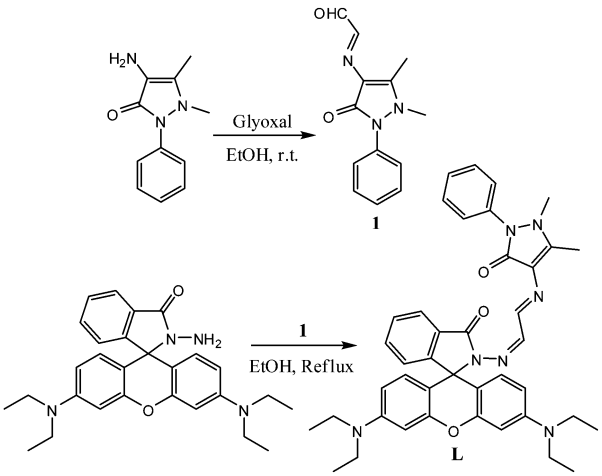

Scheme 1 The synthetic route of chemosensor **L**.

All the photophysical properties were tested in CH_3CN/H_2O (4 : 1, v/v, 10 mM HEPES buffer, pH 7.4) solution. As shown in Fig. 1, the probe **L** only was colorless and showed almost no absorbance in the visible range 480–620 nm, which was attributed to the closed spirolactam form of **L** in organo aqueous solution. Upon gradual addition of Pd^{2+} to the organo-aqueous solution of probe **L**, a new visible absorption band appeared at 555 nm and increased progressively, along with an obvious color change from colorless to pink, which may be due to the formation of the spirolactam ring-open amide form of **L** on Pd^{2+} ion coordination. Moreover, color changes in the presence of Pd^{2+} suggested that probe **L** can serve as a 'naked-eye' indicator for Pd^{2+} ions. Under similar experimental conditions, no noteworthy spectral changes were found in the presence of other competitive metal cations except Al^{3+} and Cu^{2+} (Fig. S5, ESI†). Both Al^{3+} and Cu^{2+} induced a small enhancement in absorption, suggesting probe **L** can act as a selective and sensitive chemosensor for Pd^{2+} ions.

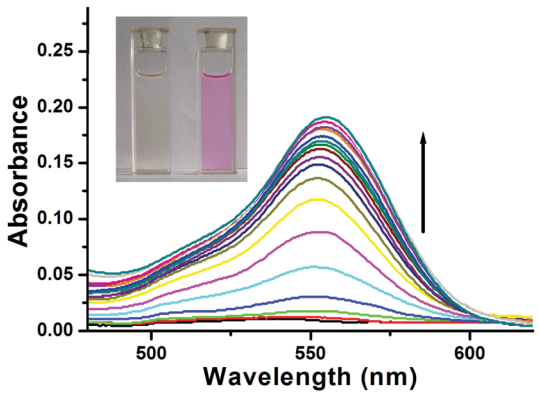

Fig. 1 The UV-vis spectral changes of probe **L** ($c = 4 \times 10^{-4}$ M) in the presence of Pd^{2+} ($c = 4 \times 10^{-5}$ M) ions in CH_3CN/H_2O (4 : 1, v/v, 10 mM HEPES buffer, pH 7.4) solution. Inset: Photographic images of **L** and **L**–Pd^{2+}.

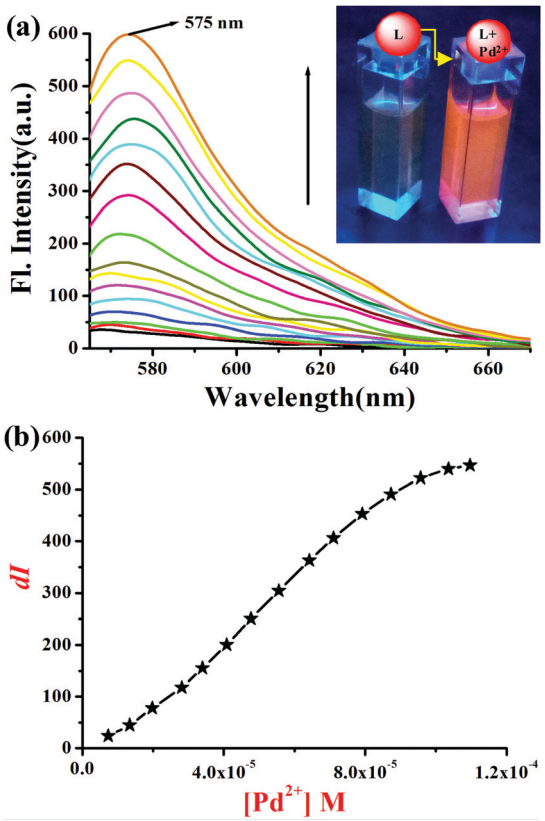

Fig. 2 Fluorescence emission spectra of **L** ($c = 4 \times 10^{-5}$ M) in aq. CH_3CN (CH_3CN/H_2O = 4 : 1, v/v, 10 μM HEPES buffer, pH = 7.4) upon addition of Pd^{2+} ($c = 4 \times 10^{-5}$ M) ions. λ_{ext} = 555 nm. Inset: Photographic fluorescence images of **L** and **L**–Pd^{2+}. Change of emission intensity at 575 nm with incremental addition of Pd^{2+} (λ_{ext} = 555 nm).

After that, we performed fluorescence titrations of probe **L** with Pd^{2+} ions in aqueous acetonitrile (4 : 1, v/v, 10 mM HEPES buffer, pH 7.4) solution. Free probe **L** showed very weak fluorescence emission upon excitation at 555 nm, indicating that the spirocyclic structure of probe **L** was predominant. However, upon addition of Pd^{2+} to the organo aqueous solution of **L**, the emission intensity at 575 nm was enhanced markedly, accompanied by visual emission color changes from colorless to orange when excited with a hand-held 365 nm UV lamp (Fig. 2). The fluorescence intensity reached its maximum after the addition of 1 equivalent of Pd^{2+} with a *ca.* 17-fold increment, which was attributed to the Pd^{2+} induced spirolactum ring opening of probe **L** to form an amide (Scheme 2).

Moreover, probe **L** displayed a good linear relationship between the emission intensity at 575 nm and the concentration of Pd^{2+} ranging from 0.02 to 0.104 mM (Fig. 2b), signifying that probe **L** is very much useful for quantitative analysis of Pd^{2+} with a wide dynamic range. Notably, the limit of detection is a critical parameter in sensor applications. From the fluorescence titration curve, the limit of detection for Pd^{2+} using the probe **L** was calculated to be 1.19×10^{-5} M (11.9 μM),[25] demonstrating that the limit of detection of **L** for Pd^{2+} is below the threshold limit for palladium content of WHO guidelines for drug chemicals [4.7×10^{-5} M (5 ppm) to 9.4×10^{-5} M (10 ppm)].[26]

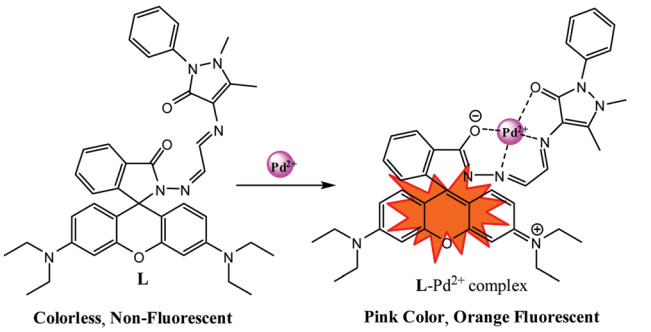

Scheme 2 Proposed sensing mechanism for the detection of Pd^{2+} by probe **L**.

To establish the stoichiometry of the complex between **L** and Pd^{2+}, a Job plot was employed and it was revealed that **L** binds with Pd^{2+} with a 1 : 1 stoichiometry (probe : metal) (Fig. S6, ESI†). The formation of a 1 : 1 complex was further confirmed by mass spectral analysis. A clear peak at *m*/*z* 788.4716 (calculated for $C_{41}H_{43}N_7O_3Pd$ = 787.2462) in the ESI-MS spectrum, assigned to [**L**–Pd^{2+}], established the formation of the 1 : 1 complex. Hence, we suggested that **L** coordinates with Pd^{2+} in a 1 : 1 manner and formed a tetracoordinate complex with the most likely binding pocket *via* carbonyl O, imino N atoms of rhodamine and antipyrene carbonyl O and inamine N. Now, from the fluorescence emission titration data, the binding constant of **L** for Pd^{2+} has been determined using the Benesi–Hildebrand equation,[27] and it was found to be $K_a = 8.36 \times 10^3$ M^{-1} (R^2 = 0.985). The binding mechanism was also verified by FTIR spectra of **L** and the **L**–Pd^{2+} complex. The peak at 1691 cm^{-1}, corresponding to the characteristic stretching frequency for the C=O amide bond of probe **L** (rhodamine unit), was shifted to 1648 cm^{-1} in the presence of 1 equivalent Pd^{2+}, showing that the amide carbonyl group is engaged in the binding event with Pd^{2+} ions (Fig. S10, ESI†).

We then proceeded to study the selectivity of probe **L** toward several metal ions (Na^+, K^+, Mg^{2+}, Ca^{2+}, Sr^{2+}, Ba^{2+}, Cr^{3+}, Mn^{2+}, Fe^{2+}, Fe^{3+}, Co^{2+}, Ni^{2+}, Cu^{2+}, Zn^{2+}, Cd^{2+}, Pb^{2+}, Hg^{2+}, Pd^{2+}, Pd^0, Pt^{2+}, Ru^{3+}, Al^{3+} and Ag^+) under the same conditions as selectivity is a very essential characteristic of an ion-selective chemosensor.

As shown in Fig. 3, only the addition of Pd^{2+} to the solution of **L** was found to display a strong fluorescence emission band centered at 574 nm, whereas no noticeable emission enhancement was caused by the other metal ions excluding Cu^{2+} and Al^{3+}, which demonstrated slight interference. Furthermore, competitive experiments were conducted by adding Pd^{2+} ions to the solution of probe **L** in the presence of various competitive metal ions and the results revealed that Pd^{2+}-induced fluorescence enhancement was unaffected by other common metal ions (Fig. S7, ESI†). From such experimental observations we can conclude that the probe **L** acts as a colorimetric and "turn-on" fluorescent probe for Pd^{2+} with remarkable sensitivity and selectivity.

To examine the binding interaction of **L** with Pd^{2+}, the optimized geometries and HOMO/LUMO energy levels of **L** and **L**–Pd^{2+}complexes, we performed density functional theory (DFT) calculations using the Gaussian09 program.[28,29] The optimized

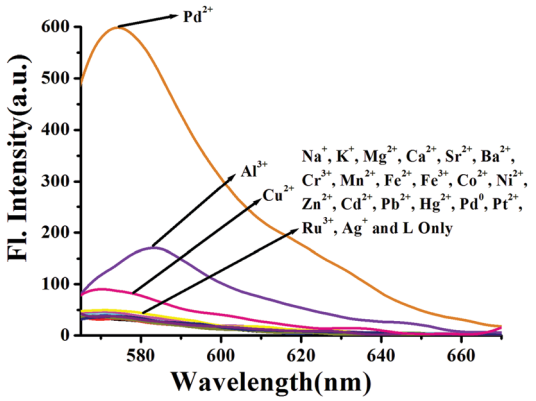

Fig. 3 Fluorescence emission spectra of **L** ($c = 4 \times 10^{-4}$ M) in the presence of different metal ions such as Na^+, K^+, Mg^{2+}, Ca^{2+}, Sr^{2+}, Ba^{2+}, Cr^{3+}, Mn^{2+}, Fe^{2+}, Fe^{3+}, Co^{2+}, Ni^{2+}, Cu^{2+}, Zn^{2+}, Cd^{2+}, Pb^{2+}, Hg^{2+}, Pd^{2+}, Pd^0, Pt^{2+}, Ru^{3+}, Al^{3+} and Ag^+ in aq. CH_3CN (CH_3CN/H_2O = 4 : 1, v/v, 10 μM HEPES buffer, pH = 7.4) solution.

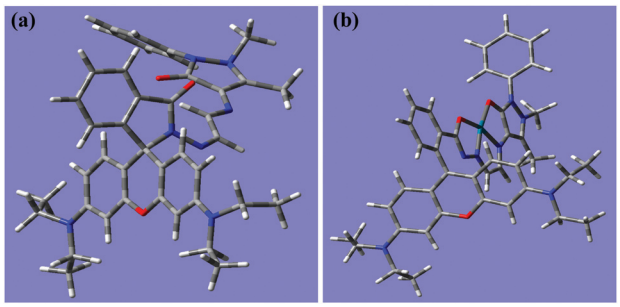

Fig. 4 The energy optimized structures of (a) **L** and (b) the **L**–Pd^{2+} complex (atom colors: gray = C, red = O, blue = N, white = H, teal blue = Pd).

geometry of **L**–Pd^{2+} is shown in Fig. 4, which illustrates that Pd^{2+} binds with **L** in a 1 : 1 fashion *via* four coordination sites (carbonyl O, imino N atoms of rhodamine and anti-pyrene carbonyl O and inamine N) and forms a tetracoordinate complex (ESI†).

The spatial distributions and orbital energies of the HOMO and LUMO of **L** and **L**–Pd^{2+} were also calculated. As depicted in Fig. 5, the π electron density on the HOMO of the **L**–Pd^{2+} complex is mostly distributed on the xanthene ring of the rhodamine platform, but the electron density on the LUMO is mainly concentrated at the centre of the guest Pd^{2+} ion. In addition, the HOMO–LUMO energy gap of the **L**–Pd^{2+} complex (1.39 eV) becomes smaller than that of the probe **L** (3.40 eV), signifying that probe **L** formed a stable palladium complex (**L**–Pd^{2+}) through four coordination sites as shown in Fig. 5.

Due to the excellent sensing properties of **L** for Pd^{2+}, the probe was then successfully applied for *in vitro* detection of Pd^{2+} ions in living MDA-MB-468 cells. However, to attain this goal, it is a prerequisite to primarily assess the cytotoxicity of probe **L** and **L**–Pd^{2+} on these living cells. The well-known MTT (3-(4,5-dimethylthiazol-2-yl)-2,5-diphenyltetrazolium bromide) assay confirmed that both **L** and **L**–Pd^{2+} were unable to exhibit any adverse effect on the cell viability of MDA-MB-468 cells, even at concentrations as high as 50 μM (ESI†). This cytotoxicity

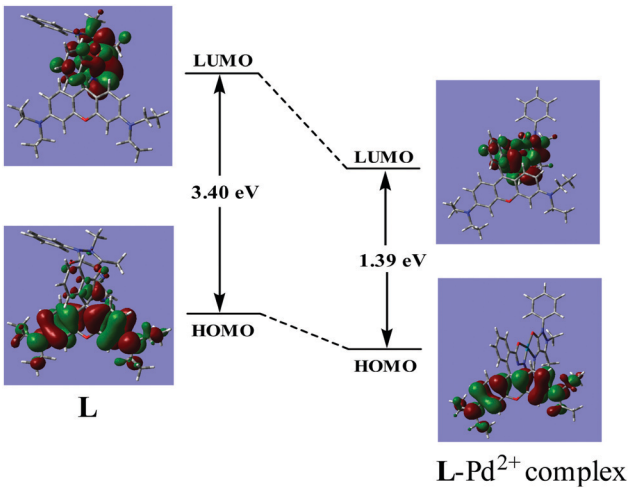

Fig. 5 HOMO and LUMO distributions of (a) **L** and (b) the **L**–Pd^{2+} complex.

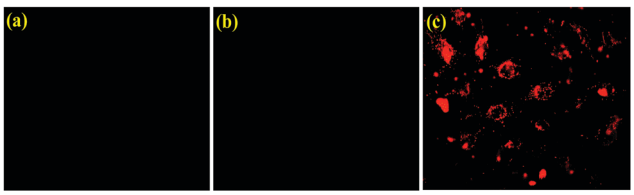

Fig. 6 Fluorescence microscopy images of MDA-MB-468 cells: (a) image of MDA-MB-468 cells treated with only $PdCl_2$ (control); (b) image of MDA-MB-468 cells treated with only probe **L**; (c) image of MDA-MB-468 cells treated with $PdCl_2$ and probe **L**.

assay revealed that probe concentrations up to 50 μM can be used for fluorescence-based bio imaging experiments of **L** and **L**–Pd^{2+} in living cells. To test the ability of **L** to image intracellular Pd^{2+} in living cells, MDA-MB-468 cells were treated with 20 μM $PdCl_2$ for 1 h followed by addition and incubation with 10 μM probe **L** solution and then imaged using a fluorescence microscope. Upon treatment with either **L** or $PdCl_2$, MDA-MB-468 cells failed to show any fluorescence, whereas a bright red fluorescence signal was observed in the cells when incubated with both **L** and Pd^{2+}, indicating the formation of the **L**–Pd^{2+} complex as already observed in solution studies. Hence, cell imaging inside the live cells suggests that probe **L** is able to permeate cell membranes and can be effectively employed for intracellular imaging of Pd^{2+} in living cells (ESI†) (Fig. 6).

Conclusions

In conclusion, we have devised a simple rhodamine derivative based chemosensor **L** for selective and sensitive detection of Pd^{2+} ions in CH_3CN–water (4 : 1, v/v, 10 mM HEPES buffer, pH 7.4) solution. Probe **L** displayed a colorimetric and "turn-on" fluorescence response towards Pd^{2+} ions resulting from the Pd^{2+} induced successive ring-opening of the spirolactum moiety, thereby providing a suitable and simple way for visual detection of Pd^{2+} ions. This newly developed probe **L** selectively detects Pd^{2+} over other commonly coexistent metal ions with a limit of detection down

to the micromolar range (11.9 μM). From fluorescence studies, the association constant for **L** with Pd^{2+} was found to be 8.36×10^3 M^{-1} indicating strong binding for Pd^{2+}. The sensitivity and selectivity of probe **L** were determined on the basis of absorption, fluorescence, FTIR and mass spectroscopy data. The Pd^{2+} binding features of probe **L** have been studied by theoretical calculations at the DFT level. Moreover, cell imaging studies revealed that probe **L** is able to permeate cells and can be employed to image intracellular Pd^{2+} ions in living MDA-MB-468 cells with low cytotoxicity.

Experimental section

Materials and equipment

All the reagents, solvents and all cationic compounds such as perchlorates of Mg^{2+}, Cu^{2+}, Fe^{2+}, Co^{2+}, Ni^{2+}, and Mn^{2+}, chlorides of Na^+, K^+, Ca^{2+}, Sr^{2+}, Ba^{2+}, Cr^{3+}, Cd^{2+}, Fe^{2+}, Zn^{2+}, Hg^{2+}, Pb^{2+}, Pd^{2+}, and Ru^{3+}, nitrate salts of Ag^+, and Al^{3+}, potassium salts of Pt^{2+}, and $Pd(PPh_3)_4$ were purchased from commercial sources, stored in desiccators under a vacuum containing self-indicating silica, and used without any additional purification. For NMR spectra, $CDCl_3$ was used as a solvent with TMS as an internal standard. Chemical shifts are expressed in ppm (δ) units. UV-visible spectra were measured on a SHIMADZU UV-1800 spectrophometer. Fluorescence spectra were recorded on a PerkinElmer LS-55 spectrofluorometer. ^{1}H NMR and ^{13}C NMR spectra were recorded on a Bruker 300 MHz instrument. Mass spectra were obtained with a HRMS QTOF Micro YA263 mass spectrometer. The following abbreviations are used to describe spin multiplicities in ^{1}H NMR spectra: s = singlet; d = doublet; t = triplet; and m = multiplet.

General technique of UV-vis and fluorescence titration studies

All experiments were carried out in CH_3CN/H_2O (CH_3CN/H_2O = 4 : 1, v/v, 10 μM HEPES buffer, pH = 7.4) solution. Solutions of 4×10^{-4} M salts of the respective cations were prepared in Millipore water. During titration, chemosensor solutions (4×10^{-5} M) were placed each time in a quartz optical cell of 1.00 cm optical path length and the metal ion stock solutions were added to the quartz optical cell progressively by using a micropipette. Spectral data were recorded 1 min after the addition of the metal ions.

Calculations for the limit of detection

The limit of detection of **L** for Pd^{2+} was determined using the following equation:

$$\text{limit of detection} = 3Sb1/S \quad (1)$$

where Sb1 is the standard deviation of the blank solution and S is the slope of the calibration curve.

Computational methods

All geometries for **L** and **L**–Pd^{2+} were optimized by density functional theory (DFT) calculations using the B3LYP functional with the 6-311G (d,p) basis set for **L** and the LanL2DZ basis set for **L**–Pd^{2+}. All calculations were carried out with the Gaussian09 software package.

Cell imaging experiments

Minimum inhibitory concentration (MIC). The antibacterial activity of compound (**L**) was affirmed through determination of the minimum inhibitory concentration (MIC). The MIC is defined as the lowest concentration of an antimicrobial agent at which no growth is observed in broth medium. Test tubes containing 3 ml of LB broth were inoculated with overnight cultures of the bacteria and then various concentrations of compound **L** (0–150 μM) were added to each tube. The tubes were left shaking at 37 °C for 24 h. Absorbances of each solution were then measured at 600 nm for the determination of bacterial growth.

Cell survivability assay. The inhibition of cell growth was measured by MTT assay. In brief, cells were seeded in 96 well plates at 1×10^4 cells per well and exposed to probe **L** at different concentrations for 24 h. After incubation, cells were washed twice with 1× PBS and incubated with MTT solution (450 μg ml^{-1}) for 3–4 h at 37 °C. The resulting formazan crystals were dissolved in a MTT solubilization buffer and the absorbances were measured at 570 nm by using a microplate reader (Biotek, USA). Each point was assessed in triplicate.

Cellular imaging. To show the intracellular uptake in MDA-MB-468, the cells were grown on a cover slip for over 24 h following the reported procedure.[30] These cells and Pd-contaminated cells were then separately treated with 5 μg ml^{-1} of **L** for 24 h at 37 °C. The cells were then washed with 1× PBS. Finally, the cells were mounted on a glass slide and fluorescence images were collected from the fluorescence microscope (Leica).

Preparation of compound 1. 4-Amino antipyrine (ampyrone) (0.400 g, 1 mmol) was dissolved in 25 ml ethanol in a 50 ml flask and then 2 ml excess aqueous glyoxal (40%) was added dropwise with continuous stirring at room temperature for 6 h. The resulting precipitate was filtered, washed with ethanol, and dried in a vacuum to give the yellow solid **1** (437 mg, yield: 91%), m.p. > 200 °C.

Preparation of L. Rhodamine B hydrazide (0.40 g, 0.88 mmol) was dissolved in 5 ml ethanol with continuous stirring and then 0.213 g compound **1** (0.88 mmol) in 15 ml ethanol was added to the solution and heated to reflux for 12 h. After that, the reaction mixture was cooled to room temperature, the solvent was evaporated and the residue left was crystallized from ethanol to give yellow colored compound **L** with 84% yield (502 mg); m.p. > 250 °C. ^{1}H NMR (DMSO-d_6, 300 MHz) δ (ppm):‡ 7.88 (s, 1H), 7.77 (d, J = 7.2 Hz, 1H), 7.16–7.36 (m, 8H), 6.93 (d, J = 7.5 Hz, 1H), 6.30–6.34 (m, 4H), 6.06 (m, 2H), 3.22 (q, J_1 = 5.7 Hz, J_2 = 12.6 Hz, 8H, 4 CH_2 of ethyl groups), 2.74 (s, 3H, N–CH_3 of the pyrazole ring) 2.05 (s, 3H, CH_3 of the pyrazole ring), 1.07 (t, J = 6.6 Hz, 12H, 4 CH_3 of ethyl groups). ^{13}C NMR ($CDCl_3$, 75 MHz) δ (ppm): 10.11, 12.61, 37.79, 44.26, 66.14, 98.81, 105.56, 107.73, 122.77, 123.37, 125.79, 126.91, 127.92, 128.95, 133.58, 147.39, 148.87, 152.68, 165.59. MS (LCMS), m/z = 682.7 $[M + H]^+$; calculated for $C_{41}H_{43}N_7O_3$ = 681.3.

‡ The proton signals observed in the region from 7.88 to 6.06 ppm are assigned to aromatic and imine hydrogens (total 17H) of probe **L**.

Conflicts of interest

There are no conflicts to declare.

Acknowledgements

SM is thankful to UGC, New Delhi, India for the D. S. Kothari Postdoctoral Fellowship. SKM and SP thank Haldia Government College, Debhog for the laboratory facility.

References

1 (*a*) M. Ware, *Platinum Met. Rev.*, 2005, **49**, 190; (*b*) M. Lafrance and K. Fagnou, *J. Am. Chem. Soc.*, 2006, **128**, 16496.

2 (*a*) T. Iwasawa, M. Tokunaga, Y. Obora and Y. Tsuji, *J. Am. Chem. Soc.*, 2004, **126**, 6554; (*b*) F. Zereini, C. Wiseman and W. Püttmann, *Environ. Sci. Technol.*, 2007, **41**, 451; (*c*) K. Pyrzynska, *J. Environ. Monit.*, 2000, **2**, 99N.

3 (*a*) K. Ravindra, L. Bencs and R. Van Grieken, *Sci. Total Environ.*, 2004, **318**, 1; (*b*) S. Rauch, H. F. Hemond, C. Barbante, M. Owari, G. M. Morrison, B. Peucker-Ehrenbrink and U. Wass, *Environ. Sci. Technol.*, 2005, **39**, 8156.

4 (*a*) J. Le Bars, U. Specht, J. S. Bradley and D. G. Blackmond, *Langmuir*, 1999, **15**, 7621; (*b*) S. MacQuarrie, J. H. Horton, J. Barnes, K. McEleney, H.-P. Loock and C. M. Crudden, *Angew. Chem., Int. Ed.*, 2008, **47**, 3279; (*c*) R. M. Yusop, A. Unciti-Broceta, E. M. V. Johansson, R. M. Sánchez-Martín and M. Bradley, *Nat. Chem.*, 2011, **3**, 239.

5 (*a*) X. Chen, K. M. Engle, D. H. Wang and J. Q. Yu, *Angew. Chem.*, 2009, **121**, 5196; (*b*) K. C. Nicolaou, P. G. Bulger and D. Sarlah, *Angew. Chem., Int. Ed.*, 2005, **44**, 4442; (*c*) S. L. Buchwald, C. Mauger, G. Mignani and U. Scholzc, *Adv. Synth. Catal.*, 2006, **348**, 23; (*d*) C. M. Crudden, M. Sateesh and R. Lewis, *J. Am. Chem. Soc.*, 2005, **127**, 10045.

6 (*a*) J. S. Carey, D. Laffan, C. Thomson and M. T. Williams, *Org. Biomol. Chem.*, 2006, **4**, 2337; (*b*) S. L. Buchwald, C. Mauger, G. Mignani and U. Scholz, *Adv. Synth. Catal.*, 2006, **348**, 23.

7 (*a*) H. F. Sore, W. R. J. D. Galloway and D. R. Spring, *Chem. Soc. Rev.*, 2012, **41**, 1845; (*b*) L. F. Tietze, H. Ila and H. P. Bell, *Chem. Rev.*, 2004, **104**, 3453.

8 Y. M. Zhou, J. L. Zhang, H. Zhou, Q. Y. Zhang, T. S. Ma and J. Y. Niu, *Sens. Actuators, B*, 2012, **171–172**, 508.

9 (*a*) *International Programme on Chemical Safety, Palladium; Environmental Health Criteria Series 226*, World Health Organization, Geneva, 2002; (*b*) T. Gebel, H. Lantzsch, K. Plebow and H. Dunkelberg, *Mutat. Res., Genet. Toxicol. Environ. Mutagen.*, 1997, **389**, 183.

10 (*a*) J. Kielhorn, C. Melber, D. Keller and I. Mangelsdorf, *Int. J. Hyg. Environ. Health*, 2002, **205**, 417; (*b*) J. C. Wataha and C. T. Hanks, *J. Oral Rehabil.*, 1996, **23**, 309; (*c*) C. L. S. Wiseman and F. Zereini, *Sci. Total Environ.*, 2009, **407**, 2493; (*d*) T. Z. Liu, S. D. Lee and R. S. Bhatnagar, *Toxicol. Lett.*, 1979, **60**, 469.

11 (*a*) C. D. Spicer, T. Triemer and B. G. Davis, *J. Am. Chem. Soc.*, 2012, **134**, 800; (*b*) T. Gebel, H. Lantzsch, K. Plebow and H. Dunkelberg, *Mutat. Res., Genet. Toxicol. Environ. Mutagen.*, 1997, **389**, 183; (*c*) R. M. Yusop, A. Unciti-Broceta, E. M. V. Johansson, R. M. Sánchez-Martín and M. Bradley, *Nat. Chem.*, 2011, **3**, 239.

12 (*a*) C. E. Garrett and K. Prasad, *Adv. Synth. Catal.*, 2004, **346**, 889; (*b*) J. A. Marcusson, *Contact Dermatitis*, 1996, **34**, 320; (*c*) J. Kielhorn, C. Melber, D. Keller and I. Mangelsdorf, *Int. J. Hyg. Environ. Health*, 2002, **205**, 417.

13 (*a*) J. S. Carey, D. Laffan, C. Thomson and M. T. Williams, *Org. Biomol. Chem.*, 2006, **4**, 2337; (*b*) U. Jappe, B. Bonnekoh and H. Gollnick, *Contact Dermatitis*, 1999, **40**, 111.

14 (*a*) C. E. Garrett and K. Prasad, *Adv. Synth. Catal.*, 2004, **346**, 889; (*b*) J. Jiang, H. Jiang, W. Liu, X. Tang, X. Zhou, W. Liu and R. Liu, *Org. Lett.*, 2011, **13**, 4922.

15 (*a*) K. Van Meel, A. Smekens, M. Behets, P. Kazandjian and R. Van Grieken, *Anal. Chem.*, 2007, **79**, 6383; (*b*) C. Locatelli, D. Melucci and G. Torsi, *Anal. Bioanal. Chem.*, 2005, **382**, 1567; (*c*) K. V. Meel, A. Smekens, M. Behets, P. Kazandjian and R. V. Grieken, *Anal. Chem.*, 2007, **79**, 6383.

16 (*a*) B. Dimitrova, K. Benkhedda, E. Ivanova and F. Adams, *J. Anal. At. Spectrom.*, 2004, **19**, 1394; (*b*) J. S. Aulakh and A. K. Malik, *Crit. Rev. Anal. Chem.*, 2005, **35**, 71; (*c*) M. Bergeron, M. Beaumier and A. Hébert, *Analyst*, 1991, **116**, 1019.

17 H. Li, J. Fan and X. Peng, *Chem. Soc. Rev.*, 2013, **42**, 7943.

18 (*a*) L. P. Duan, Y. F. Xu and X. H. Qian, *Chem. Commun.*, 2008, 6339; (*b*) L. Fabbrizzi, M. Licchelli, P. Pallavicini, A. Perotti, A. Taglietti and D. Sacchi, *Chem. – Eur. J.*, 1996, **2**, 75; (*c*) L. P. Duan, Y. F. Xu and X. H. Qian, *Chem. Commun.*, 2008, 6339.

19 (*a*) B. K. Pal and M. S. Rahman, *Mikrochim. Acta*, 1999, **131**, 139; (*b*) A. Tamayo, L. Escriche, J. Casabo, B. Covelo and C. Lodeiro, *Eur. J. Inorg. Chem.*, 2006, 2997; (*c*) X.-Z. Chen, X.-D. Ma, H.-M. Wang, M. Wang, Y.-Y. Zhang, G. Gao, J.-J. Liu and S.-C. Hou, *New J. Chem.*, 2017, **41**, 8026.

20 P. T. Matthew, D. Pham and K. Koide, *Chem. Soc. Rev.*, 2015, **44**, 4769–4791.

21 (*a*) A. K. Mahapatra, S. K. Manna, K. Maiti, S. Mondal, R. Maji, D. Mandal, S. Mandal, M. R. Uddin, S. Goswami, C. K. Quah and H.-K. Fun, *Analyst*, 2015, **140**, 1229; (*b*) S. Sun, B. Qiao, N. Jiang, J. Wang, S. Zhang and X. Peng, *Org. Lett.*, 2014, **16**, 1132; (*c*) X. Wang, Z. Guo, S. Zhu, H. Tian and W. Zhu, *Chem. Commun.*, 2014, **50**, 13525.

22 (*a*) S. Goswami, D. Sen, N. K. Das, H.-K. Fun and C. K. Quah, *Chem. Commun.*, 2011, **47**, 9101; (*b*) B. Liu, H. Wang, T. Wang, Y. Bao, F. Du, J. Tian, Q. Li and R. Bai, *Chem. Commun.*, 2012, **48**, 2867; (*c*) B. Qiao, S. Sun, N. Jiang, S. Zhang and X. Peng, *Dalton Trans.*, 2014, **43**, 4626.

23 (*a*) A. K. Mahapatra, S. K. Manna, D. Mandal and C. D. Mukhopadhyay, *Inorg. Chem.*, 2013, **52**, 10825; (*b*) A. K. Mahapatra, S. K. Manna, S. K. Mukhopadhyay and A. Banik, *Sens. Actuators, B*, 2013, **183**, 350; (*c*) A. K. Mahapatra,

S. K. Manna, K. Maiti, R. Maji, C. D. Mukhopadhyay, D. Sarkar and T. K. Mondal, *RSC Adv.*, 2014, **4**, 36615.

24 (*a*) R. Zhang, F. Yan, Y. Huang, D. Kong, Q. Ye, J. Xu and L. Chen, *RSC Adv.*, 2016, **6**, 50732; (*b*) H. N. Kim, M. H. Lee, H. J. Kim, J. S. Kim and J. Yoon, *Chem. Soc. Rev.*, 2008, **37**, 1465; (*c*) H. Zheng, X.-Q. Zhan, Q.-N. Bian and X.-J. Zhang, *Chem. Commun.*, 2013, **49**, 429.

25 (*a*) S. Mondal, S. K. Manna, K. Maiti, R. Maji, S. S. Ali, S. Manna, S. Mandal, M. R. Uddin and A. K. Mahapatra, *Supramol. Chem.*, 2017, **29**, 616; (*b*) L. Long, D. Zhang, X. Li, J. Zhang, C. Zhang and L. Zhou, *Anal. Chim. Acta*, 2013, **775**, 100; (*c*) T. Mandal, A. Hossain, A. Dhara, A. A. Masum, S. Konar, S. K. Manna, S. K. Seth, S. Pathak and S. Mukhopadhyay, *Photochem. Photobiol. Sci.*, 2018, **17**, 1068.

26 (*a*) H.-X. Wang, Y.-H. Lang, H.-X. Wang, J.-J. Lou, H.-M. Guo and X.-Y. Li, *Tetrahedron*, 2014, **70**, 1997; (*b*) S. Cai, Y. Lu, S. He, F. Wei, L. Zhao and X. Zeng, *Chem. Commun.*, 2013, **49**, 822.

27 (*a*) C. Yang, L. Liu, T. W. Mu and Q. X. Guo, *Anal. Sci.*, 2000, **16**, 537; (*b*) Y. Shiraishi, S. Sumiya, Y. Kohno and T. Hirai, *J. Org. Chem.*, 2008, **73**, 8571; (*c*) H. A. Benesi and J. H. Hildebrand, *J. Am. Chem. Soc.*, 1949, **71**, 2703.

28 (*a*) C. Lee, W. Yang and R. G. Parr, *Phys. Rev. B: Condens. Matter Mater. Phys.*, 1988, **37**, 785; (*b*) A. D. Becke, *J. Chem. Phys.*, 1993, **98**, 5648; (*c*) B. Miehlich, A. Savin, H. Stoll and H. Preuss, *Chem. Phys. Lett.*, 1989, **157**, 200.

29 M. J. Frisch, G. W. Trucks, H. B. Schlegel, G. E. Scuseria, M. A. Robb, J. R. Cheeseman, G. Scalmani, V. Barone, B. Mennucci, G. A. Petersson, H. Nakatsuji, M. Caricato, X. Li, H. P. Hratchian, A. F. Izmaylov, J. Bloino, G. Zheng, J. L. Sonnenberg, M. Hada, M. Ehara, K. Toyota, R. Fukuda, J. Hasegawa, M. Ishida, T. Nakajima, Y. Honda, O. Kitao, H. Nakai, T. Vreven, J. A. Montgomery, J. J. E. Peralta, F. Ogliaro, M. Bearpark, J. J. Heyd, E. Brothers, K. N. Kudin, V. N. Staroverov, T. Keith, R. Kobayashi, J. Normand, K. Raghavachari, A. Rendell, J. C. Burant, S. S. Iyengar, J. Tomasi, M. Cossi, N. Rega, J. M. Millam, M. Klene, J. E. Knox, J. B. Cross, V. Bakken, C. Adamo, J. Jaramillo, R. Gomperts, R. E. Stratmann, O. Yazyev, A. J. Austin, R. Cammi, C. Pomelli, J. W. Ochterski, R. L. Martin, K. Morokuma, V. G. Zakrzewski, G. A. Voth, P. Salvador, J. J. Dannenberg, S. Dapprich, A. D. Daniels, O. Farkas, J. B. Foresman, J. V. Ortiz, J. Cioslowski and D. J. Fox, *Gaussian 09, Revision D.01*, Gaussian, Wallingford, CT, 2013.

30 (*a*) A. R. Chowdhuri, D. Laha, S. Pal, P. Karmakar and S. K. Sahu, *Dalton Trans.*, 2016, **45**, 18120; (*b*) J. Mandal, P. Ghorai, K. Pal, P. Karmakar and A. Saha, *J. Lumin.*, 2019, **205**, 14.